Least-squares reverse time migration: towards true amplitude imaging and improving the resolution

S. Dong, J. Cai, M. Guo, S. Suh, Z. Zhang, B. Wang and Z. Li, TGS*

Summary

A 3D inversion based Least-Squares Reverse Time Migration (LSRTM) technique was developed. The algorithm uses the RTM as the forward modeling and inversion engine to minimize the amplitude differences between the observed data and the synthetic modeled data. In turn, the final LSRTM will deliver the reflectivity model that will generate the true corresponding amplitude; the migration artifacts are suppressed as well since they are not contained in the observed field data. Compared with the initial RTM image, the LSRTM images from the synthetic data and field data examples show the improved amplitude response and higher resolution gained by suppressing migration artifacts and sharpening the subsurface reflectors' reflectivity.

Introduction

RTM is commonly used for imaging complex structures. It provides reliable structural information of the subsurface because it is based on the full solution of the two-way wave equation. The most common RTM imaging condition is to cross-correlate the forward propagated source wavefield with the backward propagated receiver wavefield. The RTM image constructed from this imaging condition does not correspond to the geological reflectivity. The image also contains amplitude distortions caused by RTM crosstalk artifacts.

In 1993 Schuster proposed an inversion based least-squares migration (LSM) on cross-well data . In 1999 Nemeth et al. applied this technique to surface data. Their study shows that the LSM scheme can noticeably reduce migration artifacts and improve lateral spatial resolution. However, their forward modeling and migration engine is Kirchhoff migration. Recently, one-wave wave equation and two-way RTM were used as modeling and migration engine (Tang, 2008; Dai et al., 2011).

The LSM can be implemented in either model space domain (Tang, 2008; Aoki et al., 2009; Dai et al., 2011) or time domain (Tang et al., 2009; Dai et al., 2010; Zhan et al., 2010). The model space domain approach tries to solve the Hessian matrix, in turn only needing a few migration iterations, but it requires a lot of memory to solve the inversion of the Hessian matrix. In practice the Hessian matrix is too big for currently available computer power; many have tried to address this issue by approximating the Hessian matrix (Tang, 2008; Dai et al., 2011). For the time domain approach, there is less memory requirement, but multiple migration iterations are needed to solve the inversion problem. In order to save the migration iterations, the idea of blending data was proposed (Tang et al., 2009; Dai et al., 2011).

Besides the memory requirement and computation cost, there are still some fundamental issues which need to be addressed for the practical application. Considering the current computation architecture, we chose the time domain approach and used RTM as the engine for the forward modeling and migration. In this paper, we will share some practical lessons learned for LSRTM from our study.

Theory

The forward modeling operator that relates the reflectivity model *m* to scattered seismic data *d* can be represented by

$$d = Lm \qquad (1)$$

where, $\boldsymbol{L}$ represents the forward modeling operator. The migration operator is the adjoint of the forward modeling and can be represented by (Claerbout, 1992):

$$m_{mig} = L^T d \qquad (2)$$

where, m_{mig} is the migration image. To obtain a better reflectivity image, the imaging problem can be represented as a least-squares inversion problem. The solution is obtained by minimizing the objective function ***p(m)***, which is defined as the least-squares difference between the forward modeled data and the recorded data d_0:

$$p(m) = \| Lm - d_0 \| \qquad (3)$$

The iterative solution is:

$$m^{k+1} = m^k - \alpha L^T [L(m^k) - d] \qquad (4)$$

where, α is the optimized step length, $\boldsymbol{k}$ is number of iterations and L^T is the migration operator. This equation is an iterative approach for LSRTM in the data domain. It is actually a process that repeatedly projects the difference between the modeled data and the input data to the model domain, in order to adjust the reflectivity image. In this paper, the Born modeling technique was used to generate modeled data from the image.

This procedure is shown in the flow chart in Figure 1. The conventional RTM is the first approximation of the LSRTM reflectivity model. The reflectivity model is used to generate synthetic modeled data. This step is actually a de-migration by using Born modeling. Data residual is

DOI http://dx.doi.org/10.1190/segam2012-1488.1

calculated by subtracting synthetic data from the field data. Next, the gradient is calculated by using conventional RTM with the data residual. The gradient is used to adjust the reflectivity model. This procedure will be repeated until a certain data residual level is reached. Therefore, for each iteration of LSRTM, one RTM and one forward modeling step needs to be run.

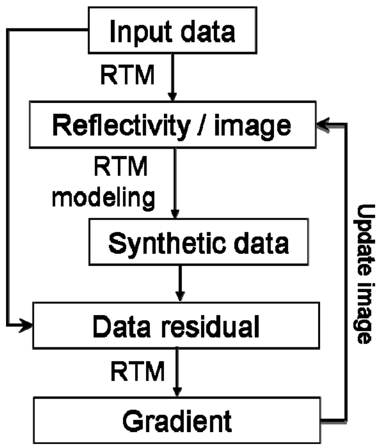

Figure 1: Work flow of LSRTM.

Synthetic data example

To validate this technique, the 2D Marmousi model with reflectivity (Figure 2A) was used. A marine streamer acquisition is simulated for the synthetic data recording. The synthetic data set is generated with the finite difference solution of the acoustic wave equation with a 20 Hz Ricker source wavelet. To simplify the problem, we use the same wave equation solver and source wavelet for the RTM and the LSRTM. This simplifies the LSRTM on the data residual calculation by avoiding the source wavelet and wave propagation difference between the input data and modeled data. Figure 2C shows the LSRTM image after the 20^{th} iteration compared with the RTM image (Figure 2B). Notice that since the LSRTM tries to solve the reflectivity model, the final LSRTM solution is higher resolution compared to the RTM image. The lateral resolution in LSRTM is also improved so fault images become sharper.

The LSRTM also suppresses migration artifacts, such as migration swings and low frequency noise. This is because during the LSRTM iterations, the artifacts in images will generate fake events in the modeled data, which do not exist in the input data. Thus the fake events will generate the negative migration artifacts in the residual gradient, and in turn the artifacts will be canceled during the gradient updating process. We also observed that the amplitude of the LSRTM image is closer to the true reflectivity.

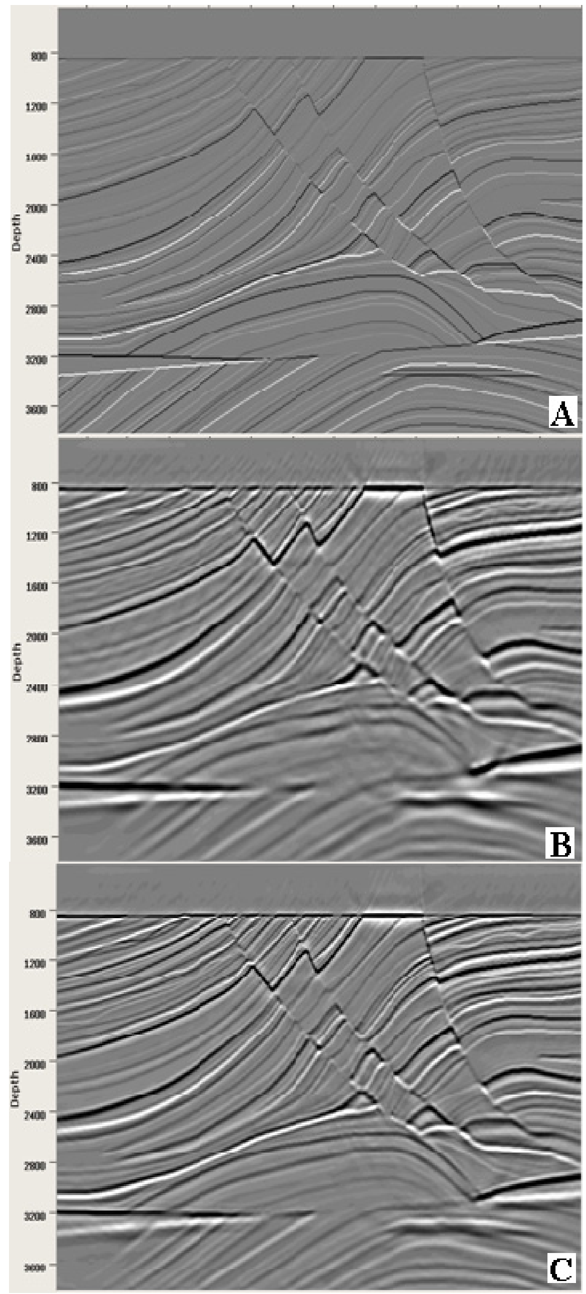

Figure 2: (A) Marmousi reflectivity model. (B) RTM image of Marmousi synthetic data by (C) LSRTM image after 20 iterations.

Data residual level and convergence rate are good indicators for LSRTM quality. Figure 3 shows the data

DOI http://dx.doi.org/10.1190/segam2012-1488.1

residual for one shot gather after 20 iterations. The most dominant results are removed. Figure 4 shows the convergence rate for 20 iterations of LSRTM. The residual levels reduce very fast for the first several iterations, and the rate slows for later iterations. This indicates that the dominant events can be matched well between the synthetic data and the input data within first few iterations.

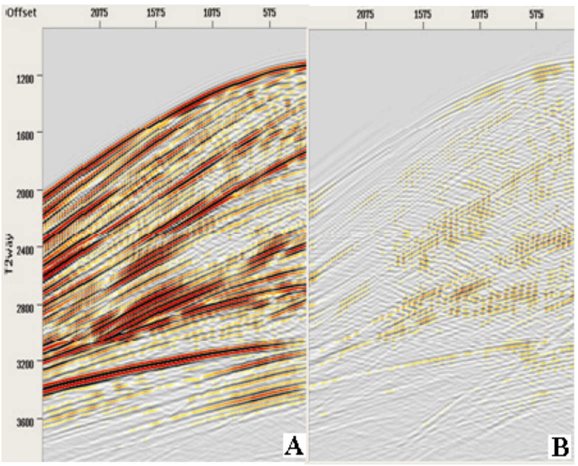

Figure 3: (A) One shot gather of synthetic input data (B) Data residual of LSRTM for the 20th iteration.

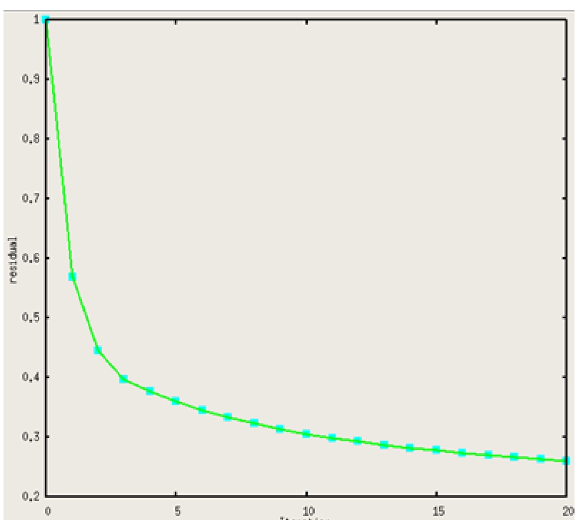

Figure 4: Data residual convergence rate for first 20 iterations. The data residual is normalized by original input data..

Getting correct data residual is a key step for successful LSRTM. However, in practice the data subtraction is not trivial. There are several issues that need to be considered for data residual calculation.

Field data practice

Even though the synthetic example provided very encouraging results, there are still many obstacles which need to be overcome for practical applications. To get more insight, we need to revisit the equations listed above. In order to minimize the objective function ***p(m)*** described in Equation 3, we need the right side of Equation 1 (***Lm***) to be able to reproduce the field data d_0, which is not easy to do. For example, the real earth is much more complex than current commonly used wave propagation media. To avoid obtaining the wrong image, routine RTM preprocessing will still be needed. For example if we use acoustic RTM, the visco-elastic property of the earth cannot be simulated by our synthetic data generator. In turn, several modes, such as converted waves will be absent from the synthetic, modeled data. Thus these modeled modes will need to be removed during processing.

In the meantime, the amplitude of the synthetic data is dependent upon the user defined source strength, which usually cannot match the real data for long wavelengths. Fortunately, for the LSRTM approach the amplitudes are different at the wavelet level, and only these differences should be used to tune up the images. Thus proper scaling of the synthetic data is needed for data residual calculation.

Deciding which type of source wavelet to use is another challenge. In the ideal case, LSRTM prefers a consistent source wavelet; therefore, proper preprocessing on field data, such as deconvolution and reshaping source wavelets, is needed. Also, we need to ensure the field data and synthetic data have a similar frequency range, by filtering both of them. Therefore, for practical application, Equation 3 needs to be modified as

$$p(m) = \| p_m Lm - p_F d_0 \|$$

where p_m indicates the preprocessing of and proper scaling and filtering of the synthetic data to match the observed field data. p_F is the preprocessing for the observed field data.

Another important issue which needs to be addressed is the velocity; since in practice the velocity error is unavoidable. The good news is that if we assume the migration and forward modeling are adjoint procedures, and the same the velocity model is used, the kinematic errors should be minor in the time domain where the data residual is calculated. Unfortunately for complex structure, velocity

DOI http://dx.doi.org/10.1190/segam2012-1488.1

errors could introduce defocusing and in turn introduce the mismatch between the synthetic modeled data and the observed field data.

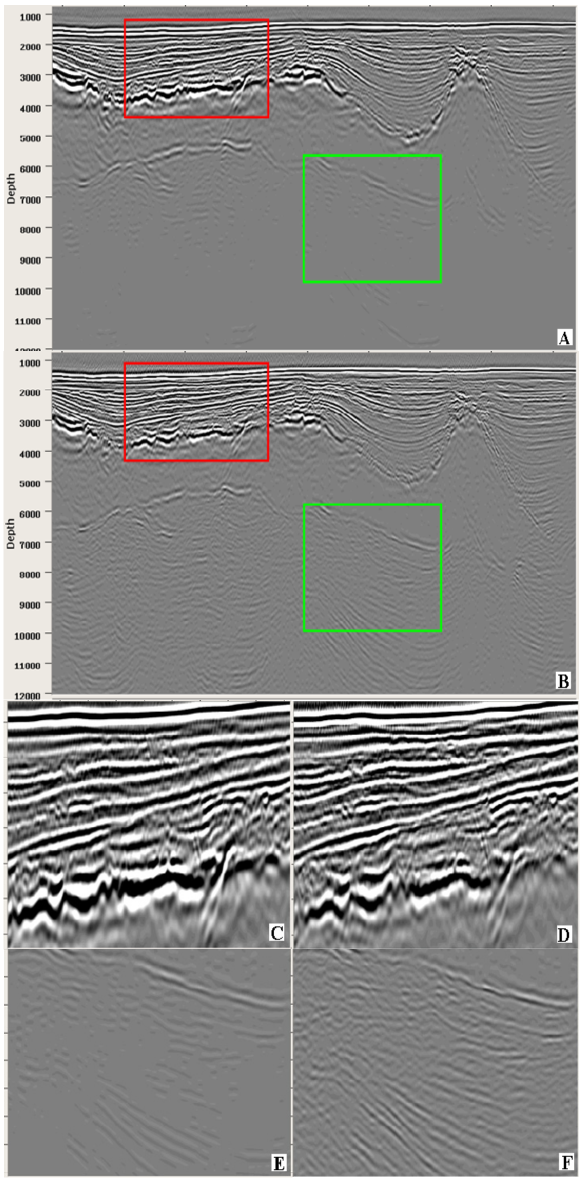

Figure 5: Migration results of a field data set from the Gulf of Mexico: (A) Conventional RTM. (B) LSRTM after 10 iterations. (C) Zoom-in view of RTM image in shallow part marked with red box in (A). (D) Zoom-in view of LSRTM image in shallow part marked with red box in (B). (E) Zoom-in view of RTM image in shallow part marked with green box in (A). (F) Zoom-in view of LSRTM image in shallow part marked with green box in (B).

Both RTM and LSRTM algorithms are applied on a field data set from the Gulf of Mexico. Salt structure introduces challenges for salt boundaries and subsalt images. The RTM image is shown in Figure 5A. Due to poor illumination, the sediments below the salt are poorly imaged. The LSRTM image after 10 iterations (Figure 5B) shows improvement in the subsalt images; and the apparent amplitudes of the subsalt reflectors are more closely aligned with the geological reflectors (Figure 5F). At the shallow part of the conventional RTM image (Figure 5C), some areas are not imaged well, due to the acquisition footprint. In the LSRTM image (Figure 5D), the survey footprints are removed and the amplitudes are more balanced.

Conclusion

A time domain, production-ready 3D LSRTM is developed. From both the synthetic and field data examples shown here, LSRTM is proven to be useful in providing close to true amplitude reflectivity images; in turn improving the image resolution and suppressing the migration artifacts. The true amplitude reflectivity and high resolution result make this algorithm very attractive for certain key imaging uses, such as reservoir monitoring and 4D seismic processing. Run time is the major challenge for LSRTM. More works need to be done to increase the convergence rate.

Acknowledgments

The authors would like to thank Ge Zhan for valuable discussion during his internship at TGS. We also thank Xuening Ma, Jean Ji and Aimin Cao for their valuable contributions during the project. We thank the management of TGS for permission to publish this paper.

DOI http://dx.doi.org/10.1190/segam2012-1488.1

http://dx.doi.org/10.1190/segam2012-1488.1

EDITED REFERENCES

Note: This reference list is a copy-edited version of the reference list submitted by the author. Reference lists for the 2012 SEG Technical Program Expanded Abstracts have been copy edited so that references provided with the online metadata for each paper will achieve a high degree of linking to cited sources that appear on the Web.

REFERENCES

Aoki, N., and G. T. Schuster, 2009, Fast least-squares migration with a deblurring filter: Geophysics, **74**, no. 6, 83–93.

Claerbout, J., 1992, Earth soundings analysis: Processing versus inversion: Blackwell Scientific Publications, Inc.

Dai, W., C. Boonyasiriwat, and G. T. Schuster, 2010, 3D multisource least-squares reverse-time migration: 80th Annual International Meeting, SEG, Expanded Abstracts, **29**, 3120–3124.

Dai, W., X. Wang, G. T. Schuster, 2011, Least-squares migration of multisource data with a deblurring filter: Geophysics, **76**, no. 5, 135–146.

Nemeth, T., C. Wu, and G. T. Schuster, 1999, Least-squares migration of incomplete reflection data: Geophysics, **64**, 208–221.

Schuster, G. T., 1993, Least-squares crosswell migration: 63rd Annual International Meeting, SEG, Expanded Abstracts, **12**, 25–28.

Tang, Y., 2008, Wave-equation Hessian by phase encoding: 78th Annual International Meeting, SEG, Expanded Abstracts, **27**, 2201–2205.

Tang, Y., and B. Biondi, 2009, Least-squares migration/inversion of blended data: 79th Annual International Meeting, SEG, Expanded Abstracts, **28**, 2859–2863.

Zhan, G., and G. T. Schuster, 2010, Skeletonized least-squares wave equation migration: 80th Annual International Meeting, SEG, Expanded Abstracts, **29**, 3380–3384.